Chapter 1

Formation of Nanolayer on Surface of EPD Coatings Based on Poly-Ether-Ether-Ketone

Maria Federica De Riccardis

Additional information is available at the end of the chapter

http://dx.doi.org/10.5772/67570

Abstract

Poly-ether-ether-ketone (PEEK) is a high performance polymer with many intrinsic properties. When it is used in the form of coating, an improvement of some of its functional properties was achieved by forming a surface nanolayer. In this chapter, it will be described how it was possible to obtain this result. Firstly, three kinds of PEEK composite coatings were deposited by electrophoretic deposition, adding alumina particles, polytetrafluoroethylene (PTFE) and lignin to PEEK. Then, the composite coatings were thermal treated in a furnace. Therefore, surface nanostructure and chemical composition of these PEEK composite coatings were modified with respect to bulk coatings, due to interaction between PEEK chain and secondary phase, emphasised by the thermal treatment conditions. Experimental evidence of the formation of surface nanolayer was provided by SEM, TEM, GIXRD, ATR-FTIR and XPS characterisations. Functional characterisations demonstrated that wear resistance—in the presence of alumina particles—hydrophobicity—in the presence of PTFE—and corrosion resistance—in the presence of Lignin—were increased with respect to pure PEEK.

Keywords: nanolayers PEEK, wear, friction coefficient, corrosion, EPD

1. Introduction

Poly-ether-ether-ketone (PEEK) is a high performance polymer with excellent mechanical, chemical and thermal properties. It is a polyaromatic semicrystalline thermoplastic polymer (typically with 30–40% crystallinity), formed by three benzene rings and a carbonyl group (**Figure 1**). In form of a coating, PEEK can be used continuously up to 260°C, is insoluble in all common solvents, is characterised by a low moisture absorption, and shows a low outgassing.

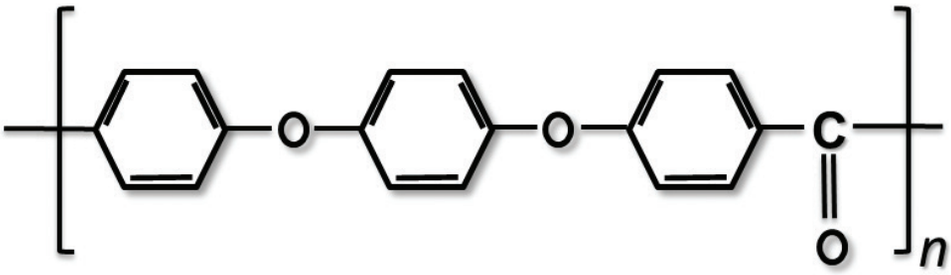

Figure 1. PEEK chemical structure.

In spite of its outstanding properties, PEEK exhibits some drawback. As an example, it has a high friction coefficient in dry sliding, therefore tribology applications are restricted. Nevertheless, several application limits can be overcome adopting some expedient during or after processing, aiming to modify surface nanostructure or creating a thin surface layer, as demonstrated by some examples cited below.

As for nanostructure, excellent properties of PEEK are partly the result of its semi-crystalline structure developed during processing [1–3], therefore a variation of the processing temperature could result in improved mechanical interactions between its surface and surroundings, such as in tribology or anticorrosive applications.

For some biomedical applications, native PEEK film was found to be a very poor substrate of cell cultivation, extremely reluctant to allow cellular adhesion. Improvement of the bioadhesion properties could possibly result from an increase of the surface hydrophilicity, for instance by the introduction of carboxyl groups or by UV irradiation. In such a way, these reactive surface functionalisations should be excellent anchorage points for the immobilization of bioactive molecules [4–6].

Moreover, it is well noted that pure PEEK results is limited in osteoconduction and osseointegration resulting in a poor biocompatibility. To achieve good bone-implant interfaces, the surface properties of permanent implants made of PEEK could be modified, acting on morphology and chemical structures of the surface [7, 8]. In the review [9], different physical modifications of PEEK, used to improve the bone implant interface are described. These modification methods include forming a bioactive layer by coating technology and changing the surface properties by wet treatment.

In general and from all these considerations on PEEK, it is evident that the surface of a bulk material, or better its thin superficial layer, plays a fundamental role in interactions between a material and working ambient. It is worthwhile to note that these modifications are at nanoscale level, but nevertheless they can influence the macroscopic properties of a material. For this reason, it is reasonable to study how to modify a material, and in particular the physical or chemical structure of its surface, to improve some peculiar characteristics. Specifically for PEEK, experimental results demonstrated that its outstanding properties or structures related to surface were improved by adding a secondary phase. The aim of this chapter is to illustrate the interesting results obtained for thin layers of PEEK in terms of some properties related to surface, such as friction coefficient, wear resistance and hydrophobicity.

http://dx.doi.org/10.5772/67570

2. Deposition process

The deposition technique used to obtain thin layers based on PEEK was Electrophoretic Deposition (EPD). It is one of the most outstanding coating techniques based on electrodeposition that does not induce polymer degradation with respect to other deposition techniques such as thermal spraying or printing processes.

Although EPD usually is used to obtain coating some microns thick, it was demonstrated that by performing a post-deposition treatment with opportune parameters, or by using some kind of secondary phase together with PEEK, it was possible to obtain a nanoscale surface layer with modified characteristics able to improve the outstanding properties of bulk material.

EPD is a method traditionally employed to obtain ceramic coatings. Nowadays, both academics and industrialists are more and more interested in it, due to its wide potential in coating processing technology, also applied to polymer and composite coatings. EPD coating process consists in applying an electric field between two electrodes immersed in a suspension where some solid particles or polymer chain are present. The particles or the polymer chains inside the liquid medium of the suspension acquire a surface charge, also for effect of additives or stabilisers added to the suspension. When the electric field is on, it enables a movement of particles towards the electrode with opposite charge. There, the nanoparticles or the polymer chains coagulate and form a thin layer covering the electrode (**Figure 2**).

The main advantages of this deposition technique are high versatility and cost effectiveness. Indeed, EPD can be used with different materials or their combinations and requires simple and cheap equipment. Moreover, it can be used both on a large scale, also when coating objects with a complex geometrical form, and on a small scale, to fabricate composite micro- and nanostructures. New application areas for EPD are the low-cost fabrication of composite

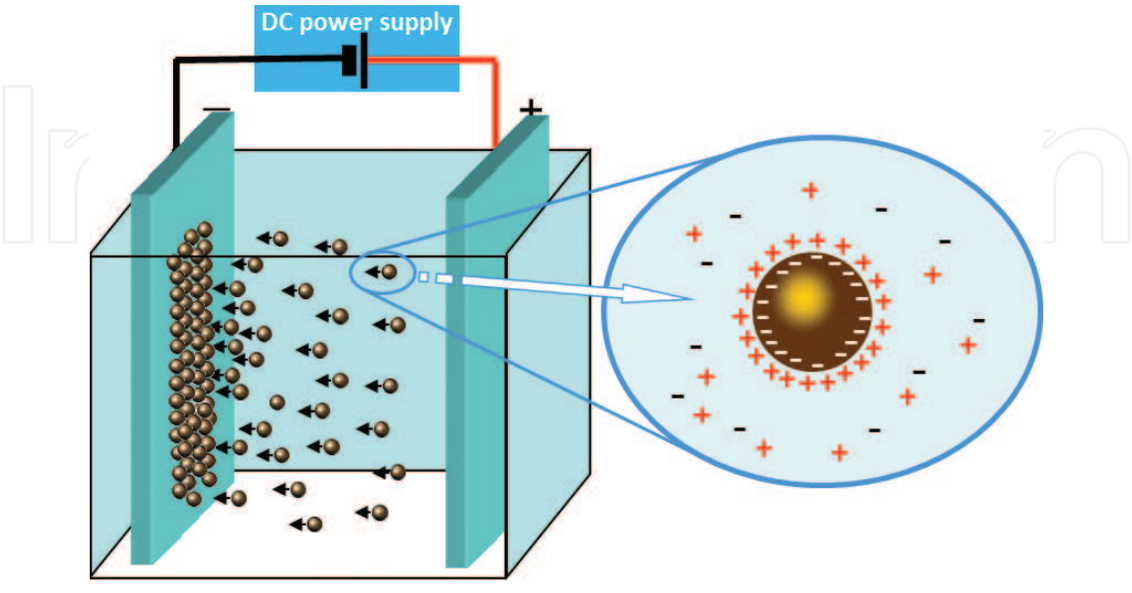

Figure 2. Scheme of an EPD cell.

materials including advanced coatings based on nanocomposites, laminate structures and functional graded materials [10–13].

It is clear that the main requirement to obtain an efficient EPD process is to use suitable suspensions where particles or other components, also at nano scale, are well suspended and dispersed. When a particle is in a liquid medium, it can be charged through four mechanisms [14]:

a. selective adsorption of ions onto the solid particle from liquid,

b. dissociation of ions from solid phase into the liquid,

c. adsorption or orientation of dipolar molecules at the particle surface and

d. electron transfer between the solid and the liquid phase due to the difference in work function.

Usually, the stability of a suspension is evaluated by means of zeta potential measurements, referring to the chemical surroundings of a particle while it is in a suspension; when the zeta potential value is maximised, with positive or negative value indifferently, the dispersion of suspension components is good and a uniform coating can be obtained by EPD.

For the analysis and discussion on charging mechanisms and particles interactions, that are at the base of this processing method, one can refer to the fundamentals of colloid science widely discussed in literature [15].

In this chapter, the experimental data regarding three different composite layers based on PEEK will be reported.

The first kind of composite PEEK coatings contains alumina particles, the most used ceramic material in the field of anti-wear application. These composite layers were prepared in order to obtain coatings with higher wear resistance than the pure PEEK without altering significantly its low friction coefficient. After deposition, a thermal treatment was performed in opportune conditions, so a nanolayer of PEEK covered the alumina particles, providing an improvement in sliding properties of PEEK-alumina coating. Morphological and chemical characterisations of the surface nanolayer were conducted to investigate the interaction between polymer chains and ceramic particles in processing.

As second kind of PEEK coating, a combination of PEEK and polytetrafluoroethylene (PTFE) was prepared. Often these two polymers are used together in order to improve the friction coefficient. In this case, the process conditions were studied in order to obtain superhydrophobic nanolayers based on PEEK and PTFE, characterised by a high crystallinity. For this aim, structural and thermal investigations were conducted to pinpoint the process conditions that resulted optimal.

Finally, the third kind of PEEK based coatings was formed by using an organic additive of vegetal origin together with PEEK. In such a way, these composite coatings showed an improved adhesion to substrate. Moreover, on the surface of coatings, a thin composite layer was formed providing an improved corrosion resistance. Adhesion and corrosion tests, as

well as morphological and chemical characterisations, were fundamental in the investigation of functional properties of PEEK layers.

3. Nanolayers of PEEK on alumina particles

PEEK semicrystalline powder (Victrex® Manufacturing Ltd.) and alumina particles (AES 11 Sumitomo) were used to prepare suspensions suitable for EPD process. The weight ratio between the alumina and PEEK content, hereafter referred as to WR, was varied between 0 and 1 in the suspension, whereas the total amount of solid content was fixed at 1wt%. Ethyl alcohol was used as liquid medium and a solution of triethylamine and citric acid was added as dispersant (10wt% with respect to solid content) [16]. The zeta potential values measured on the suspensions with different composition were quite similar, meaning that the addition of alumina particles to PEEK suspension did not modify the potential efficiency of the EPD process. EPD depositions were performed at constant voltage conditions (25 V/cm applied for 30 sec) and pieces of Si wafer were used as depositing electrode. Since a drawback of the EPD is the low density of the deposit, made of particles put together by the weak van der Waals forces [17], the coatings were submitted to a post-deposition treatment. It was a conventional thermal treatment in a furnace, operated at different temperatures to reach PEEK melting.

Before post-deposition treatments, the thermal behaviour of PEEK was analysed both in absence and in presence of alumina particles. From Thermogravimetric Analysis (TGA) and Differential Scanning Calorimetry (DSC) measurements, reported in **Figure 3**, it is possible to extrapolate that PEEK is a polymer stable up to 580°C, its crystallisation temperature at 250°C, and its melting temperature at 340°C. Moreover, no significant differences in the thermal behaviour of the PEEK powder and the powder of PEEK mixed with alumina particles, in the range of temperature between 0 and 450°C, are appreciable.

For the conventional thermal treatment, two thermal programs were used with different maximum temperature and different time. The operating parameters were reported in **Table 1**. It is worthwhile to note that the samples treated at 340°C took longer time to pass through the crystallisation range (250°C) than those treated at 400°C, as it was impossible to externally control the cooling down step.

The morphology of the coatings thermally treated was very different, as demonstrated by SEM observations. In **Figure 4**, SEM images at high magnification referring to the surface of PEEK-alumina coatings with different content of alumina particles are reported. The different maximum temperature of thermal treatment and the different cooling rate allowed to obtain different nanostructure of thin PEEK layer covering the alumina particles, more rough at 340°C than at 400°C. In fact, as visible in **Figure 4a**, **c, e** and **g** a fine structure was visible on the alumina particles surface, more evident when the alumina content was lower. When the maximum temperature was higher (**Figure 4b**, **d**, **f** and **h**), the granular nanostructure on alumina particles is less visible. It is reasonable to suppose that these features are due to PEEK solidified on alumina particles, remaining at solid state, as melting temperature of alumina is much higher than the maximum temperature of thermal treatments. As a comparison, in **Figure 5**, a SEM image of alumina particles as received is reported.

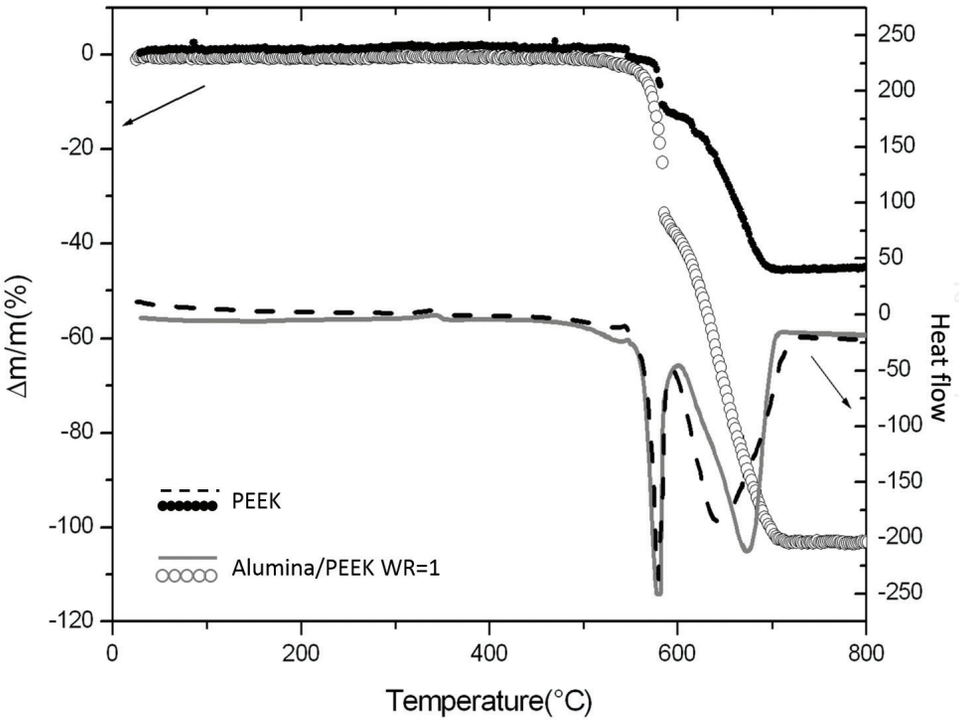

Figure 3. TGA and DSC curves conducted on pure PEEK and on PEEK-alumina powders (WR=1).

	Heating rate	Treatment time
Thermal program #1	10°C/min	30 min @340°C
Thermal program #2	10°C/min	5 min @400°C

Table 1. Operating parameters of the conventional thermal treatment conducted on PEEK-alumina layers.

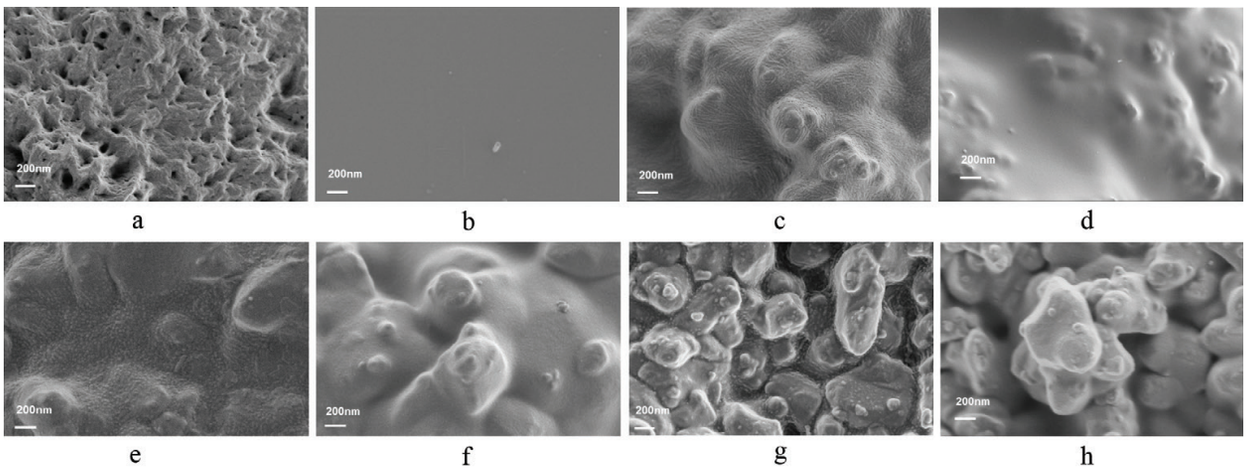

Figure 4. SEM images of fine surface structure of PEEK-alumina coating at different alumina content (a-b: WR = 0, c-d: WR = 0.3, e-f: WR = 0.7, g-h: WR = 1) treated at different temperatures (a, c, e and g @340°C, b, d, f and h @400°C).

http://dx.doi.org/10.5772/67570

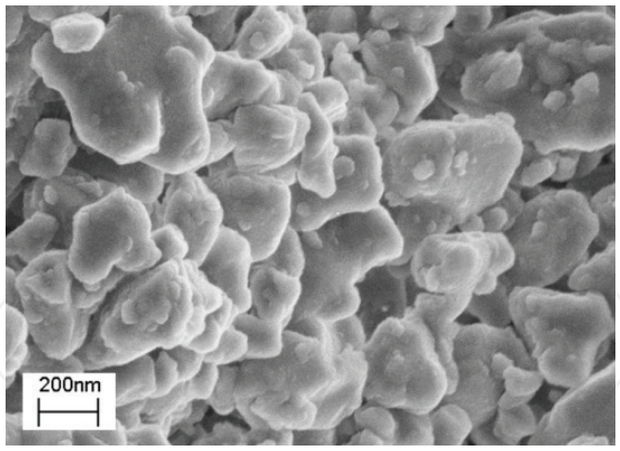

Figure 5. SEM image of alumina particles as received.

XRD measurements acquired in glancing incidence scattering configuration (GIXRD) were performed by keeping the incident angle ω_i (angle between incident beam and sample surface) fixed at 1.5°, in order to analyse surface structures. As a result, in PEEK coatings without alumina particles (WR = 0) treated at 400°C, the PEEK structure is amorphous whereas in the coatings treated at 340°C the characteristic diffraction peaks of PEEK are present (**Figure 6a**). Of course, when alumina particles are present in the coating, also the alumina peaks are visible (**Figure 6b**). Moreover, the peaks of PEEK, whose crystallites are wide 5.3 nm, are more intense when the amount of alumina is lower. In general, it is known that inorganic fillers have two inconsistent influences on the crystallization of semicrystalline polymers. On the one hand, they act as nucleating agents that facilitate the crystallisation of polymers. On the other hand, they hinder the motion of the segments of the polymer chains retarding the crystallisation of polymers. In this case, the hindering effect of alumina particles dominated.

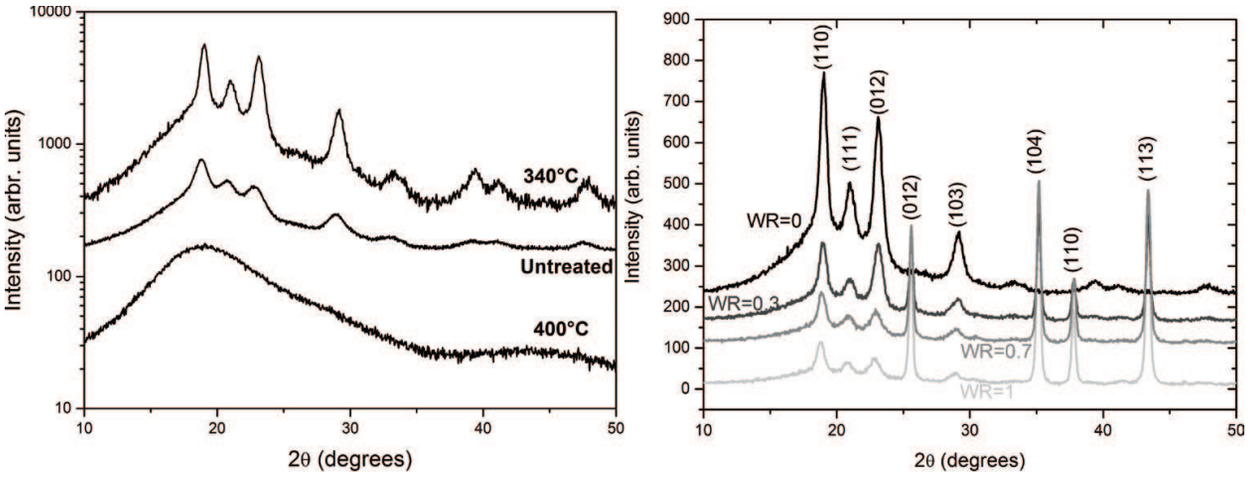

Figure 6. XRD spectra of pure PEEK coating treated at different temperature (a), and PEEK-alumina coating surface with different alumina content, after thermal treatment at 340°C (b).

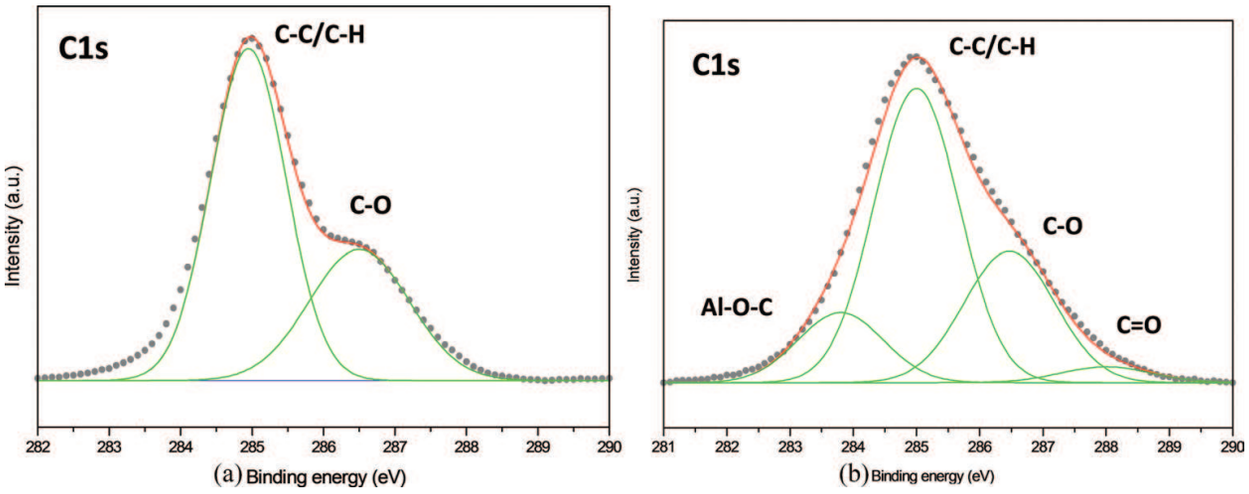

Figure 7. Deconvolution of XPS C1s signal acquired on the surface of pure PEEK coating (a) and of PEEK-alumina coating (WR = 1) (b).

The surface composition of the PEEK nanolayer was analysed by XPS measurements and the C1s peak was deeply studied. On pure PEEK, no important differences were visible in the shape of the C1s peak in layer treated at 340 and 400°C. Moreover, the thermal treatment at 340°C did not induce any significant modification in the O/C ratio with respect to untreated PEEK, but this ratio is lightly increased at 400°C, probably due to some thermal degradation of the PEEK chain.

C1s peaks acquired on surface of PEEK enriched of alumina particles were deconvoluted and different components in the binding energy signal were recognised. No particular differences were observed between C1s peak acquired on coating treated at 340°C and that of coating treated at 400°C. Therefore, the discussion is referred to C1s peak related to 340°C (**Figure 7**). On C1s peak acquired on pure PEEK, at high binding energy the C-O bond component was recognisable, less intense of the component at lower binding energy attributable to C-C and C-H bonds. The deconvolution of C1s peak of the sample PEEK with alumina particles (WR = 1), showed

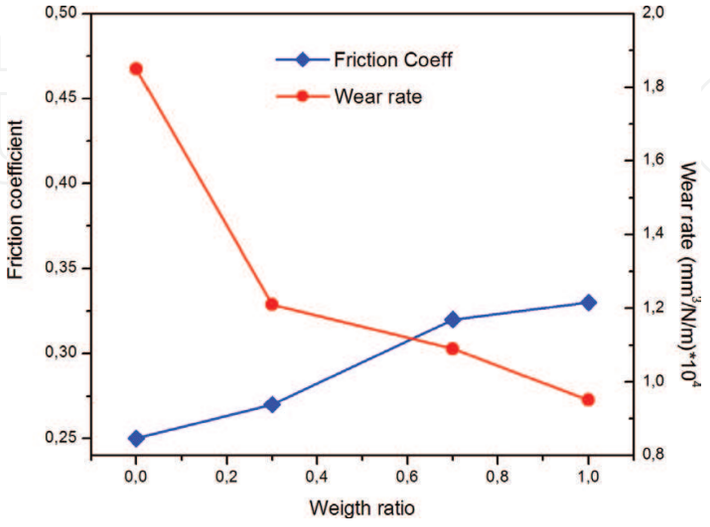

Figure 8. Friction coefficient and wear rate measured on PEEK coatings with different weight ratio between PEEK and alumina content.

the presence of a contribute of C = O and, more significantly, that of the component Al-O-C both at 340 and at 400°C, meaning that a sort of bond between PEEK and alumina was created. This result was confirmed also by the O1s signal (not reported here), that is formed by a larger peak when alumina was present.

The presence of this PEEK nanolayer on alumina particles positively affected macroscopic properties related to the surface that are friction coefficient and sliding wear. As reported in **Figure 8**, the wear rate, evaluated by means of a microtribometer (CSM), decreased when the alumina content increased. Of course, the wear rate minimum is achieved when alumina particles are present in the PEEK coating with a WR = 1. In correlation with this result, the friction coefficient increased lightly.

4. PEEK-PTFE nanolayers

As mentioned before, PEEK exhibits a high friction coefficient in dry sliding, which restricts its tribology applications. In order to reduce the friction coefficient of PEEK and therefore to increase its range of applications, some solid lubricants, such as glass and carbon fibres, graphite or carbon nanotubes [3, 18, 19, 20], as well as polymers with low surface energy, such as PTFE [21, 22], were added to the PEEK matrix. In this section, it was demonstrated that an EPD coating based on PEEK and PTFE treated in opportune condition after deposition had significant tribology properties as well as a remarkable super hydrophobicity with respect the pure PEEK coatings.

Recently, EPD has demonstrated to be a suitable method to obtain polymer coatings based on PEEK [23–26]. As regard to PTFE, to the best of author's knowledge, only few papers referred to EPD of this polymer [27, 28] and always PTFE was mixed to inorganic powders.

As first time, EPD from optimised suspensions containing PTFE and PEEK was widely discussed in reference [29]. After deposition, thermal treatments were performed in order to modify crystallinity of polymeric blend. The coatings used for this aim were indicated in **Table 2**.

DSC is the best analytical technique used for assessing polymer crystallinity, by quantifying the heat associated with melting of the polymer. It is known that, assuming that the heat

Sample	wt% PEEK	wt% PTFE
PEEK 100	100	-
MIX1	80	20
MIX2	50	50
MIX3	20	80
PTFE 100	-	100

Table 2. PEEK and PTFE content in suspension used for the EPD coatings.

capacity of a polymer is substantially independent from the temperature, it is possible to calculate the mass fraction crystallinity (χ) by evaluating the melting enthalpy from the DSC thermogram, according to the following formula:

$$\chi = \frac{H_m}{H_f} \tag{1}$$

Where, H_m is the melting enthalpy, calculated as the area under the crystal melting transition per unit weight, and H_f is the theoretical heat of fusion for a pure crystalline phase, equal to 130 J/g and 82 J/g for PEEK and PTFE, respectively. Therefore by normalizing the recorded heat value of fusion to that of a 100% crystalline sample of the same polymer, the mass fraction crystallinity was obtained.

In order to increase, and then quantify, the crystallinity of PEEK-PTFE blends, a composed DSC thermal program was used. Therefore, the PEEK-PTFE powder mixtures with composition equal to those reported in **Table 2**, were exposed to repeated processes of *heat/cool/heat*, corresponding to a melting/solidification/measuring cycle, respectively. The rates of melting and cooling processes were 1, 5, 20 and 50°C/min, whereas the second heating process was performed at 10°C/min in order to acquire a suitable thermal signal. In this way, the first heating and the low rate cooling were expected to increase polymer crystallinity. As an example, in **Figure 9**, a typical DSC-thermogram of the PEEK 50%-PTFE 50% was reported.

First of all, χ was measured on 100% PEEK and 100% PTFE powder as received, by a single heating at 10°C/min. The crystallinity of these materials was evaluated 58.0 and 94.3% for PEEK and PTFE, respectively. Some mixture of PEK-PTFE powder with the nominal composition of EPD suspensions were treated as described before. For each concentration of polymers different from 100%, the crystallinity was evaluated agreeing Eq. 1 and compared

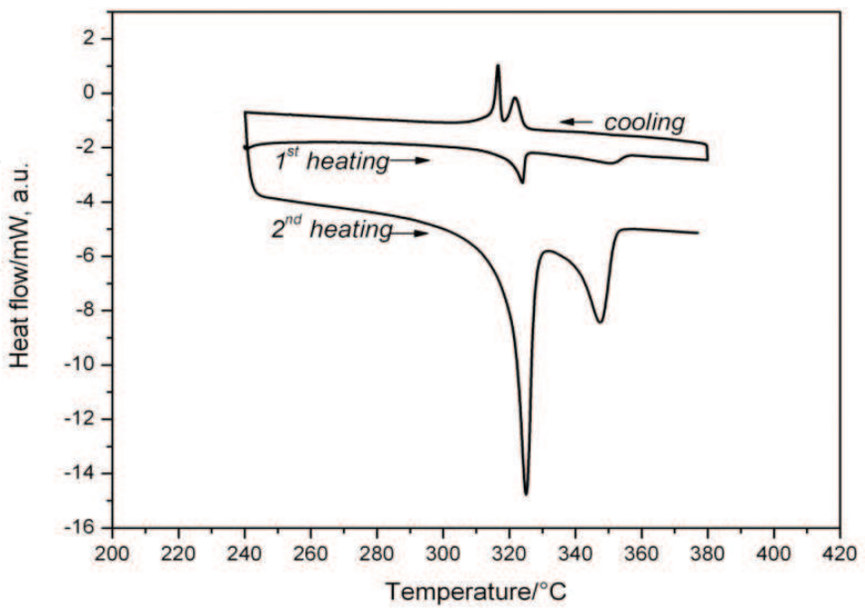

Figure 9. DSC-thermogram of the PEEK 50%-PTFE 50% cycled with 5°C/min (2nd heating = 10°C/min).

http://dx.doi.org/10.5772/67570

with the theoretical value of χ (χ_{th}), given by the ratio between the crystallinity of 100% polymer and the nominal content in the blend. In other words, for a given concentration C of PEEK

$$\chi_{th}(C) = \frac{\chi_{100}}{C} \tag{2}$$

Same evaluations were conducted for PTFE.

As first result, PEEK/PTFE blends thermal treated exhibited a different crystallinity with respect to 'as received' PEEK and PTFE, as an effect of the cooling rate. It was observed that the sample PEEK 100 treated at 1 and 5°C/min has a higher crystallinity fraction than the PEEK 'as received', whereas in presence of PTFE, χ of PEEK is lower than both the theoretical value and that 'as received' (**Figure 10**).

PTFE had a similar behaviour but the theoretical values of crystallinity fraction are significantly lower than the measured χ (**Figure 11**). Moreover, in PTFE 100, the crystallinity was higher than that 'as received' for all the thermal rate. As first conclusion, one can affirm that the presence of PTFE influenced the crystallinity of PEEK and vice versa, at a fixed value of cooling rate.

As, mentioned before, thermal treatments in DSC apparatus and consequent evaluations of fraction crystallinity were performed on mixtures of two polymer as powder, agreeing with the composition reported in **Table 1**. The successive measurements of x-ray diffraction, SEM

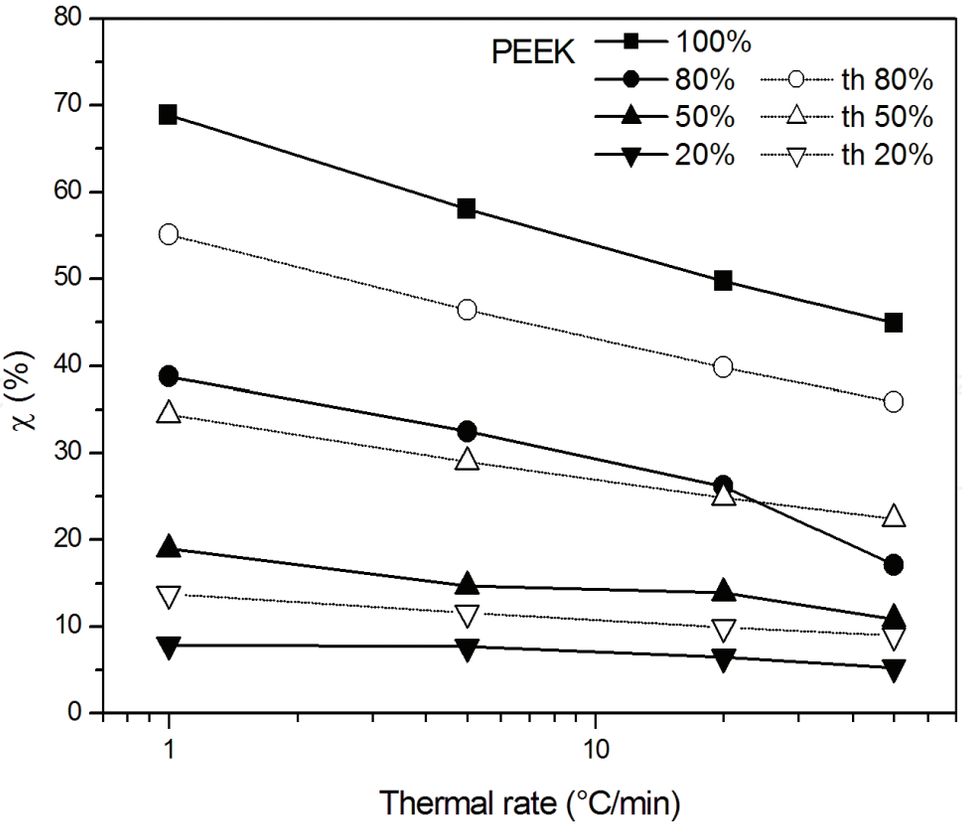

Figure 10. PEEK crystallinity evaluated at different thermal rates for different content in PEEK-PTFE blends.

and TEM observations, contact angle, friction coefficient and wear rate were performed on PEEK-PTFE coatings treated in similar conditions. Nevertheless, result discussion was consistent with DSC conclusion.

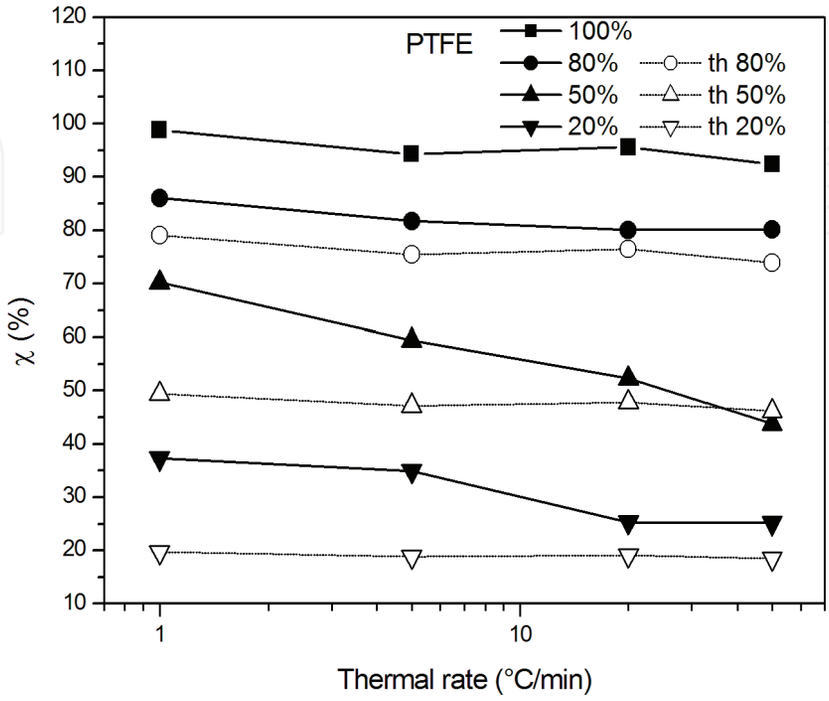

Figure 11. PTFE crystallinity evaluated at different thermal rates for different content in PEEK-PTFE blends.

XRD measurements, performed both in Bragg-Brentano configuration (θ/2θ) and in glancing-incidence configuration (GIXRD), confirmed the crystalline structure of PEEK and PTFE. Moreover, the peak intensities of PTFE were higher than those of PEEK, agreeing with DSC analysis.

SEM images at high magnification highlighted a surface morphology characterised by small granular features, recalling a fine crystalline structure (**Figure 12**). Cross section of these coatings was observed by SEM and TEM. In all coatings, a thin layer about 30 nm thick was revealed in correspondence of the surface (**Figures 13a** and **14**), sometimes detached from underlying material (**Figure 13b**). It is evident that this thin layer had a different structure with respect to the bulk of coating that appears without a structured morphology. This surface peculiarity was attributed to the interaction between first surface layer of material and ambient during cooling step.

The crystalline structure as well as the morphological features at nanoscale of the surface of these coatings conferred a super-hydrophobicity nature to PEEK. In fact, contact angle measured on PEEK-PTFE coatings was remarkably higher than that on pure PEEK surface, comparable to pure PTFE (**Figure 15**). Finally, friction coefficient and wear rate of PEEK-PTFE coatings resulted lowered with respect to pure PEEK and pure PTFE (**Figure 16**), meaning that the nanoscale layer, formed on the surface of these polymer coatings, as a consequence of carefully performed thermal treatment, resulted to have more outstanding properties than the pure PEEK.

http://dx.doi.org/10.5772/67570

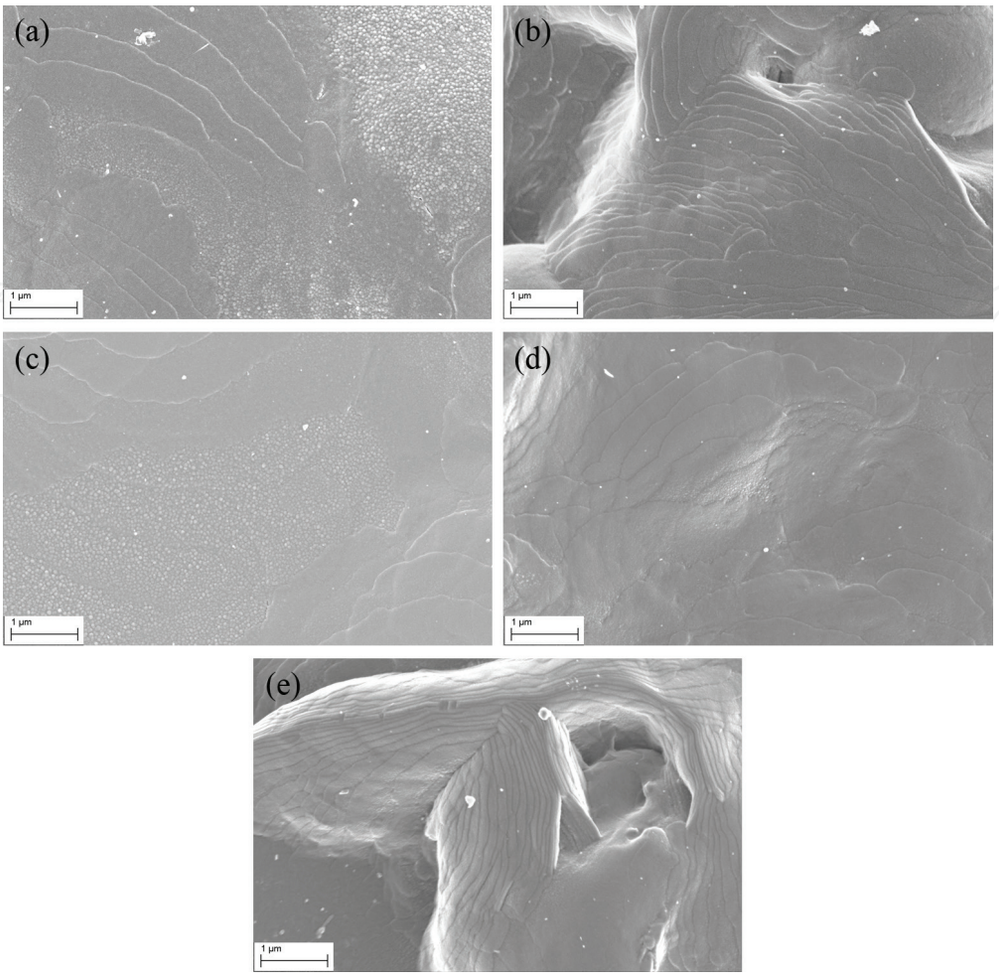

Figure 12. SEM images of fine surface structure on PEEK 100 (a), PTFE 100 (b), MIX1 (c), MIX2 (d), and MIX3 (e) coatings.

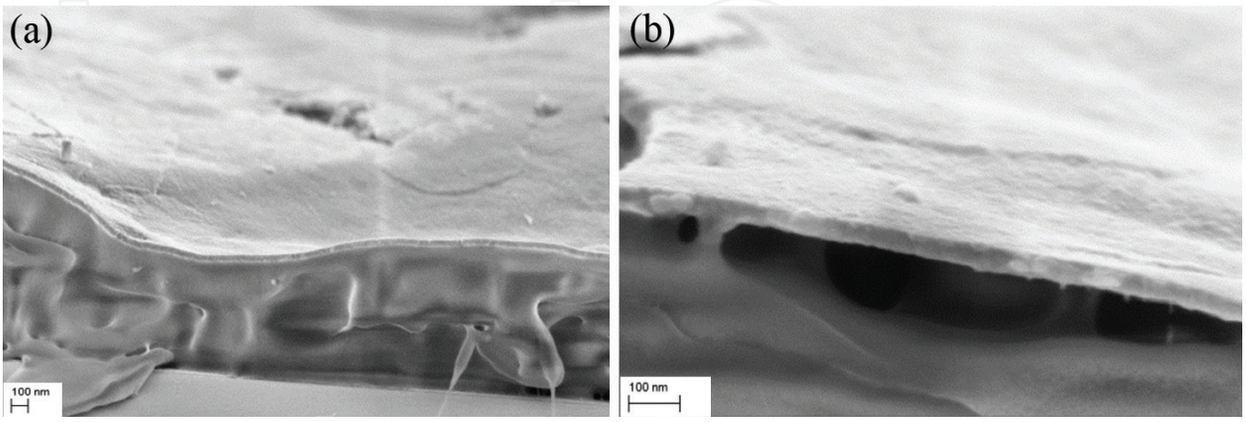

Figure 13. SEM images of cross section of a typical PEEK-PTFE coating with a thin surface layer (a). In (b) the thin layer appears detached from underlying material.

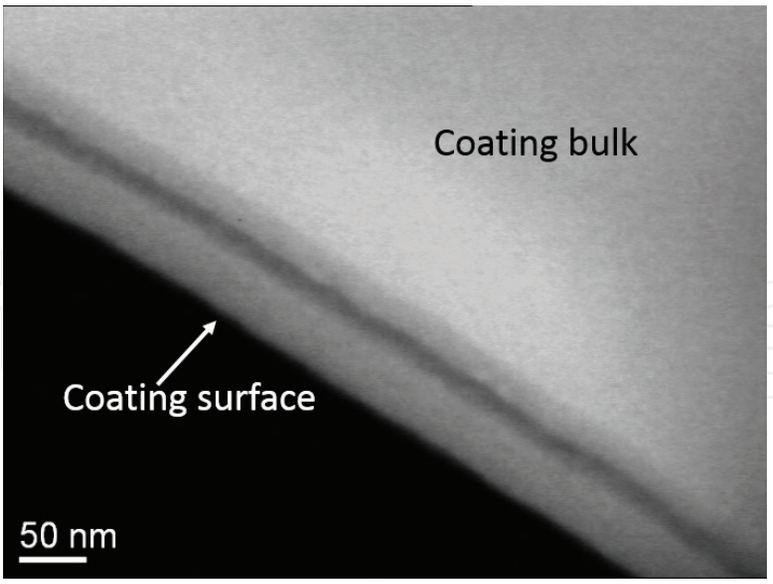

Figure 14. TEM image of thin surface layer of PEEK-PTFE coating in cross section.

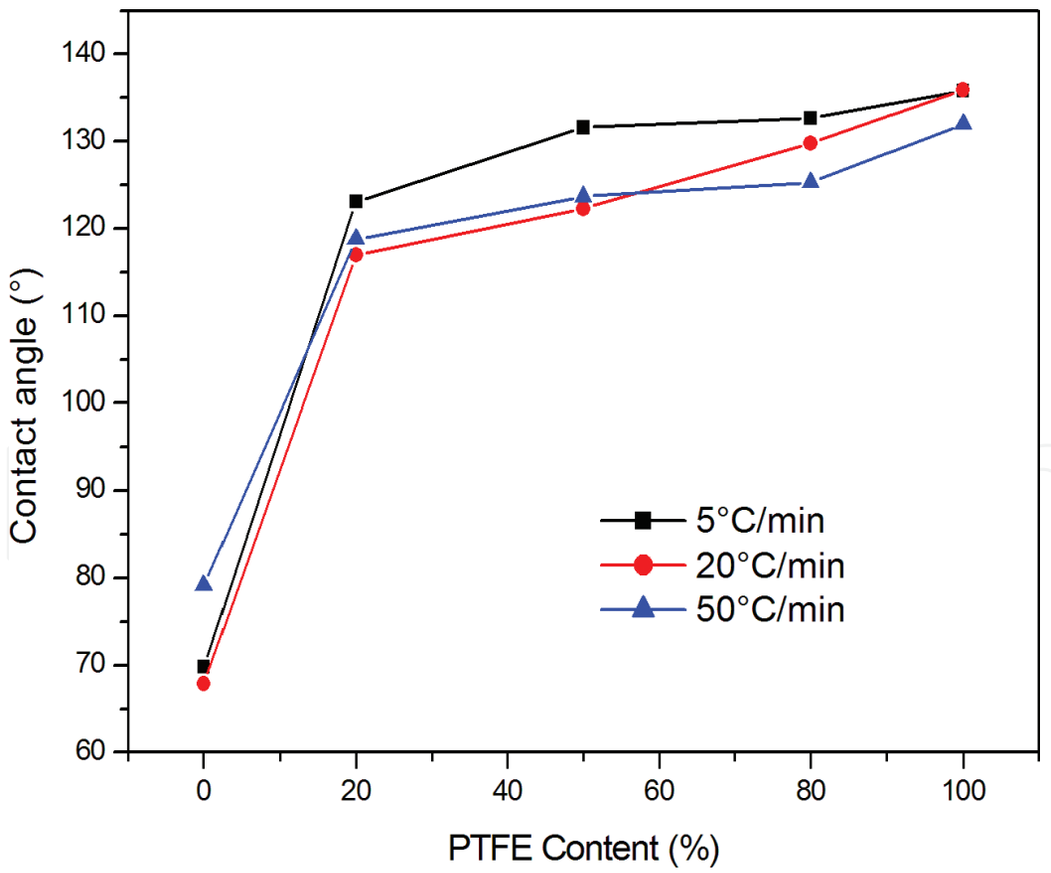

Figure 15. Contact angle measured on PEEK-PTFE coatings.

http://dx.doi.org/10.5772/67570

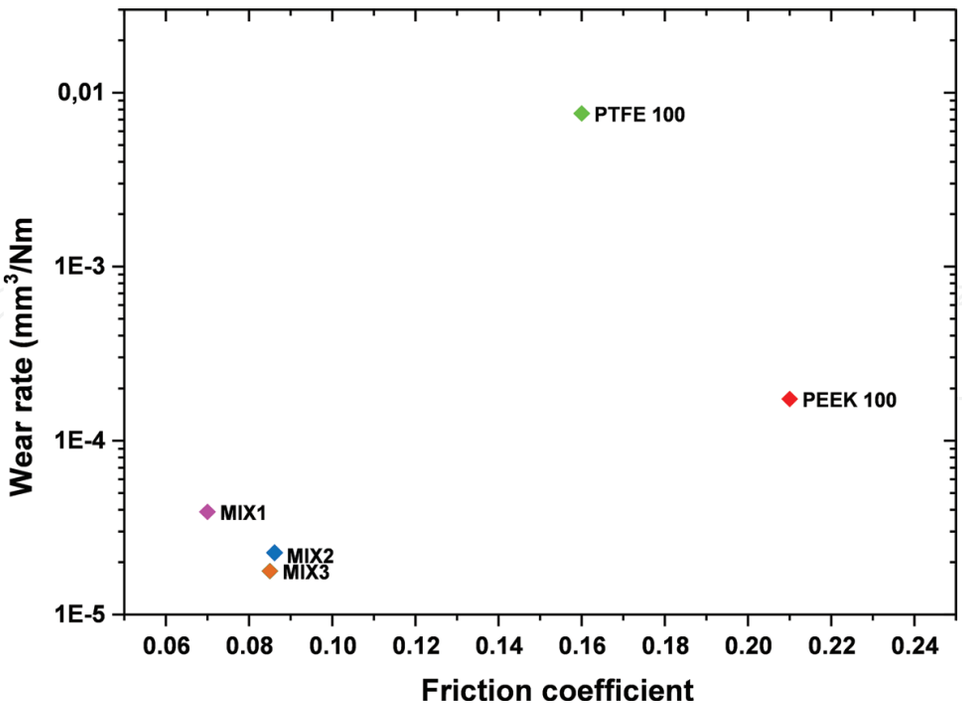

Figure 16. Friction coefficient and wear rate measured on PEEK-PTFE coatings.

5. PEEK-Lignin nanolayers

As described before, EPD has been successfully applied to obtain polymers coatings such as PTFE and PEEK, also in combination with ceramic and biocompatible particles [30]. Sometimes EPD coating adhesion to substrate is critical, principally for applications where interactions between coating surface and working environment are stressed. In order to improve the adhesion of PEEK coatings to conductive substrates, Lignin (hereafter referred as to LGN) was added to EPD PEEK suspensions. Experimental conditions and results were discussed in reference [31]. As a further result, a remarkable corrosion resistance was detected in PEEK-LGN coatings, as demonstrated by electrochemical corrosion measurements.

As an abundant non-toxic amorphous natural polymer, LGN is the second most abundant biopolymer after cellulose. It is a polymer found extensively in the cell walls of all woody plants, and constitutes 25–30% of the total dry weight of trees. LGN, formed by removal of water from sugars to create aromatic structures, resists attack by most microorganisms, and anaerobic processes tend not to attack the aromatic rings at all. Aerobic breakdown of LGN is slow and may take many days.

Due to its very complex structure, LGN has had historically a limited industrial use but the study of its properties has showed its potentiality in new value-added applications. As an example, the functional groups of LGN determine the high polarity of the macromolecular structure and make it an extremely promising material as a chemical component in polymer blends or as an organic filler. Moreover, LGN helps to lower the cost of finished products, since

it is an inexpensive by-product of the paper industry. In this specific case, LGN addition could further improve the remarkable properties of PEEK without interfering with its applications.

To investigate anticorrosion properties, some EPD coatings were prepared by using a suspension containing PEEK and LGN dispersed in acetone without further dispersant. The solid content of PEEK and LGN was fixed at 1.6 and 0.8 g/L, respectively.

LGN is a phenolic polymer with a complex structure where several chemical functional groups, including hydroxyl, methoxyl, carbonyl and carboxyl groups, are present in various amounts and proportions, depending on genetic origin and extraction processes (**Figure 17**). Differently from other solvent (deionised water, ethanol and isopropanol), when was dispersed in acetone, LGN conferred a brown colour upon acetone, meaning that some interactions between solid and liquid occurred. In order to investigate dispersion mechanism of LGN, Attenuated Total Reflection Fourier Transform Infrared Spectroscopy (ATR FT-IR) analysis was performed on LGN powder after evaporation of different solvents. By comparing the spectra acquired on as received LGN powder and on LGN residual after removing solvent (**Figure 18**), a new relevant peak at 1700 cm^{-1} appeared in LGN-Acetone, due to stretching of C=O bond. Moreover, other differences are appreciable: (1) an increase on the intensity of the broad peak due to stretching of C-H and O-H in the range 3500–3200 cm^{-1} (not reported here); (2) a general increase of peak intensity in the region 1600–1000 cm^{-1} and (3) a shift towards lower wavenumber in 1425, 1370 and 1220 cm^{-1} peaks attributed to C-H bonds [31]. These results allowed to presume that an interaction between the carbonyl group (C=O) of acetone and methyl (CH_3), methoxyl (CH_3O) or hydroxyl (OH) groups of LGN occurred and therefore LGN resulted functionalised.

After deposition on stainless steel substrates, pure PEEK and PEEK-LGN coatings were thermal treated in air at 300 and 320°C for 10 min. The morphology of the surface was quite different depending on maximum temperature of treatment, as visible in **Figure 19**. Pure PEEK appears quite rough whereas PEEK-LGN coating surface presents some small ridges, more evident at 300°C.

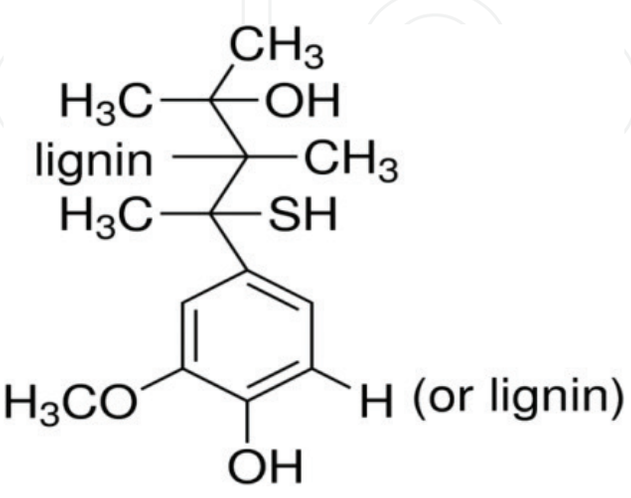

Figure 17. Lignin chemical structure.

http://dx.doi.org/10.5772/67570

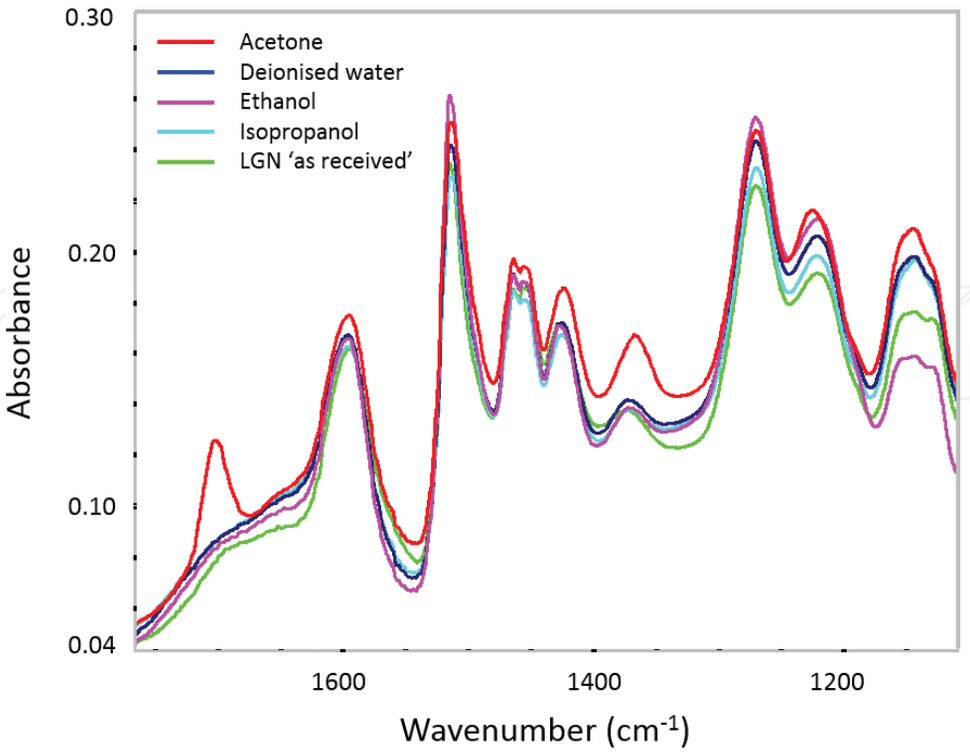

Figure 18. ATR-FTIR spectra acquired on LGN residual powder after evaporation of different solvents, compared with as received LGN.

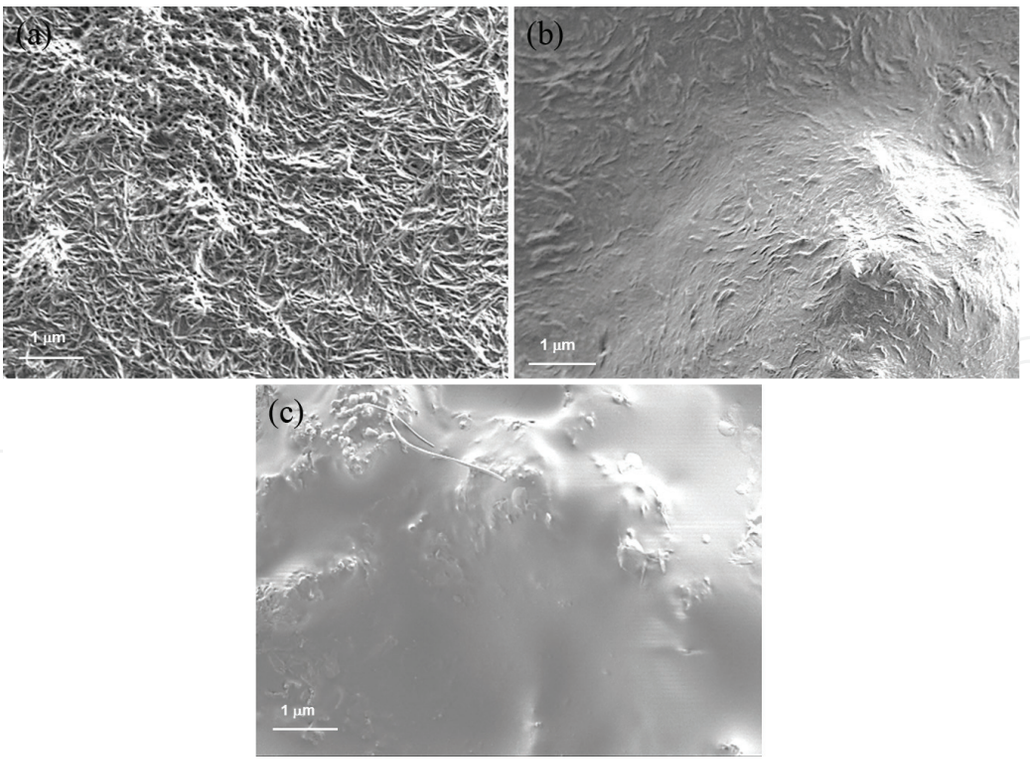

Figure 19. Surface SEM images of PEEK coating treated at 320°C (a), PEEK-LGN coating treated at 300°C (b) and at 320°C (c).

As demonstrated by TG analysis, when LGN is present together with PEEK in the deposited layers, the thermal degradation starts at lower temperature than pure PEEK (**Figure 20**). Therefore, at 320°C the PEEK-LGN layer resulted melted with a lower surface roughness.

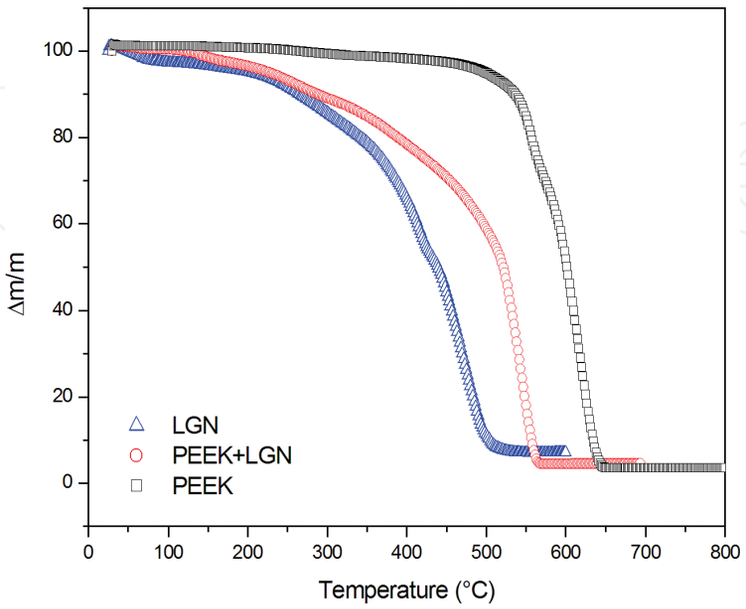

Figure 20. TG curves acquired on pure PEEK (squares), PEEK-LGN (circles) and pure LGN (triangles).

Potentiodynamic curves acquired in NaCl 3.5 g/L solution demonstrated a better anticorrosion behaviour of PEEK+LGN layers than the pure PEEK layer (**Figure 21**). Moreover, corrosion potential was higher and corrosion current was lower when PEEK+LGN layer was treated at 320°C than at 300°C (**Table 3**). This behaviour can be attributed to surface being

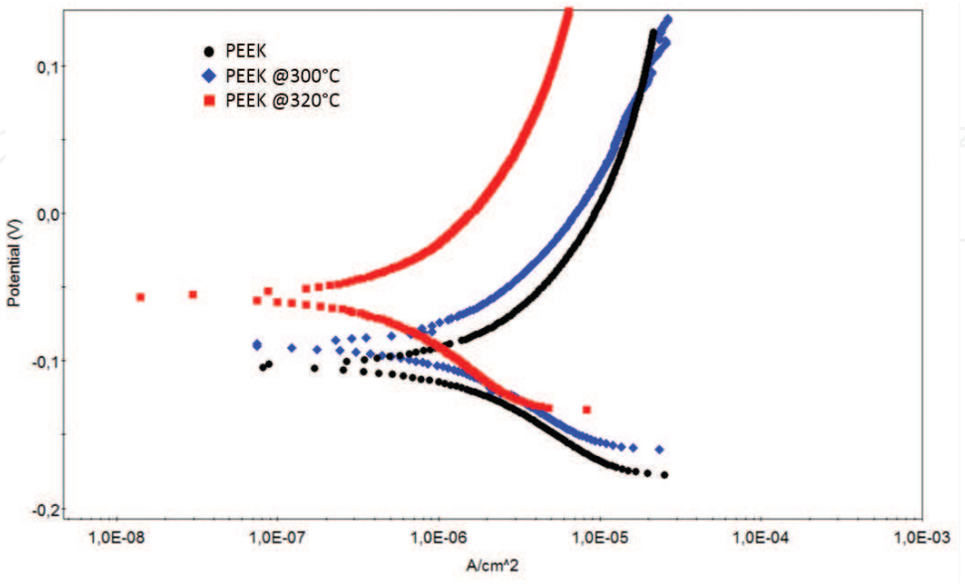

Figure 21. Potentiodynamic curves acquired on PEEK (circles) treated at 320°C and PEEK-LGN coatings in NaCl 3.5 g/L solution treated at 300°C (diamonds) and 320°C (squares) (V vs. Ag/AgCl, 10 mV/s).

characterised by a low porosity. In fact, it is well known that morphological characteristics of a layer influence electrochemical response of its surface to electrolytes interaction when the layer is immersed in an electrolytic solution [32–35].

Coating	Corrosion potential (V vs. Ag/AgCl)	Corrosion current (A/cm²)
PEEK 320°C	−0.10	1.2×10^{-6}
PEEK-LGN 300°C	−0.09	7.2×10^{-7}
PEEK-LGN 320°C	−0.05	3.4×10^{-7}

Table 3. Corrosion potential and corrosion current evaluated for PEEK and PEEK-LGN coatings.

Finally, this result was supported by electrochemical impedance spectroscopy (EIS) measurements. For EIS measurements, a small (usually 10 mV) AC signal is superimposed on the electrochemical system of interest and the system response to this perturbation is measured. The system is composed principally by electrolyte and electrolyte-coating interface and may be represented by an equivalent electrical circuit having a similar electrical behaviour. By studying the complex impedance, it is possible to identify the analysed system features.

Nyquist plot relative to PEEK layer thermally treated at 320°C is reported in **Figure 22**. As discussed in another author's work [36], PEEK layer can be electrically represented as depicted in **Figure 22**, where constant phase element (CPE) component is typical of a porous layer.

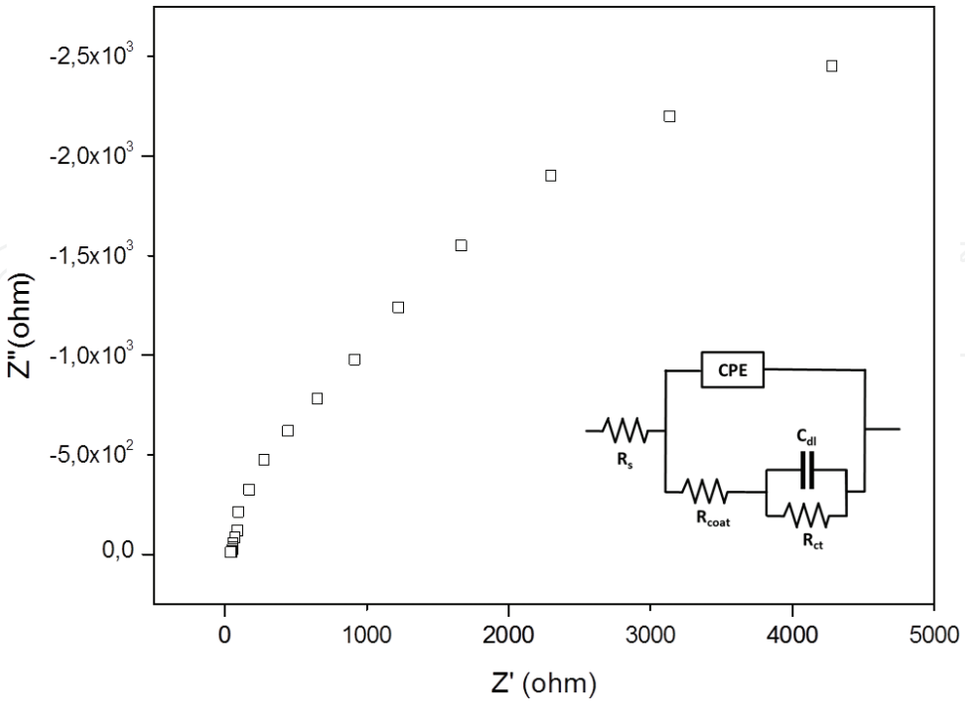

Figure 22. Nyquist plot acquired on PEEK coating treated at 320°C in NaCl 3.5 g/L solution (V vs. Ag/AgCl). In the inset is reported the equivalent circuit representing the coating.

Differently from pure PEEK layer, EIS spectra acquired on PEEK-LGN layers treated at 300 and 320°C (**Figure 23**) corresponded to an electrical circuit composed by two RC loop (inset in **Figure 23**), meaning that two layers could be recognised in the electrochemical behaviour. In other words, the PEEK-LGN-coating surface interacted in a way almost separated from the remaining layer with solution electrolytes.

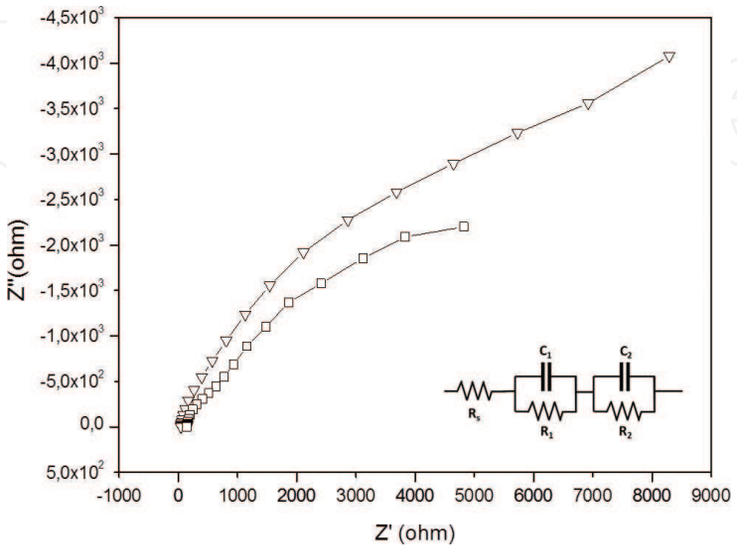

Figure 23. Nyquist plot acquired on PEEK-LGN coating treated at 300 and 320°C in NaCl 3.5 g/L solution (V vs. Ag/AgCl). In the inset is reported the equivalent circuit representing the coating.

The surface of these PEEK based layers was studied by ATR-FTIR measurements, estimating that the thickness interested to infrared analysis was lower than one micron. By comparing spectra acquired on PEEK-LGN coatings before and after thermal treatment (**Figure 24**), it is possible to note for treatments at higher temperature: (1) a lower intensity

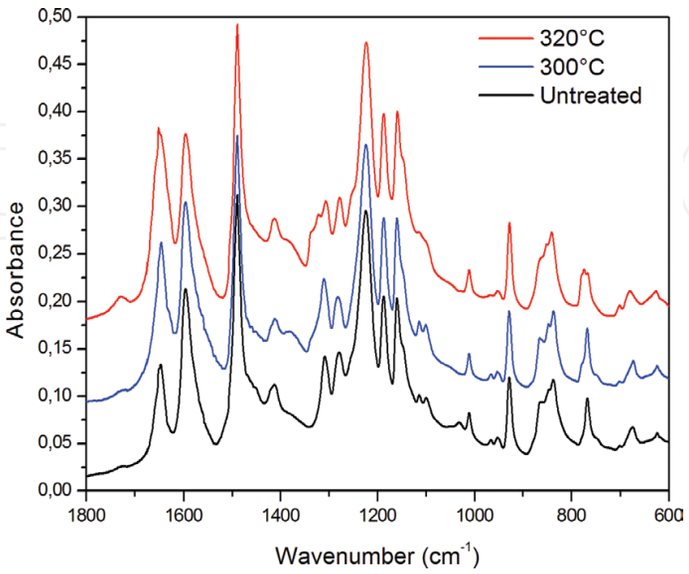

Figure 24. ATR-FTIR spectra acquired on PEEK-LGN coatings before and after thermal treatments at 300°C and at 320°.

of C-H bend stretching of aromatic ring in the range 750–900 cm^{-1}, (2) a decrease of the intensity of C-O ether bend (1300–1350 cm^{-1}), (3) a changed ratio between peak intensities of C-O-R bend stretching at 1600 and 1650 cm^{-1}. All these results, together with the decreased intensity of large band 3200–3600 cm^{-1} (not reported here), mean that an interaction between LGN and PEEK occurred on surface, promoted by temperature, probably through hydrogen bonds between functional groups of LGN and PEEK. It was demonstrated that by adding a certain amount of LGN to PEEK, the thin surface layer of PEEK-LGN coatings showed improved anticorrosion properties, attributed to morphology as well as to chemical resistance of LGN.

6. Conclusions

The outstanding properties of PEEK were further improved by creating a surface nanolayer. This interesting result was obtained by adding a secondary phase to PEEK and thermally treating the composite material based on PEEK. The starting point is EPD technique used to obtain a coating containing PEEK and the secondary phase. After deposition, the coating was submitted to thermal treatment in a conventional furnace, paying particular carefulness to controlling thermal parameters. In such a way, nanostructure or chemical composition of the surface nanolayer was modified with respect to bulk material. As a result, physical and chemical interactions with working ambient produced an improved macroscopic functional behaviour of PEEK.

Author details

Maria Federica De Riccardis

Address all correspondence to: federica.dericcardis@enea.it

ENEA-Italian National Agency for New Technologies, Energy and Sustainable Economic Development, SSPT-PROMAS-MATAS, Brindisi, Italy

References

[1] Liu T, Mo Z, Wang S, Zhang H. Non isothermal melt and cold crystallisation kinetics of poly(aryl-ether ether ketone ketone). Polymer Engineering and Science. 1997;**37**:568–575. doi:10/1002/pen.11700.

[2] Hamdan S, Swallowe G. Crystallinity in PEEK and PEK after mechanical testing and its dependence on strain rate and temperature. Journal of Polymer Science Part B: Polymer Physics.1996;**34**:699–705. doi:10.1002/(SICI)1099-0488(199603)34:4.

[3] Zhang G, Schlarb A K. Correlation of the tribological behaviors with the mechanical properties of poly-ether-ether-ketones (PEEKs) with different molecular weights and their fiber filled composites. Wear. 2009;**266**:337–344. doi:10.1016/j.wear.2008.07.004.

[4] Henneuse C, Goret B, Marchand-Brynaert J. Surface carboxylation of PEEK film by selective wet-chemistry. Polymer. 1998;**39**(4):835–844. doi:10.1016/S0032-3861(97)00362-5.

[5] Henneuse-Boxus C, Dulière E, Marchand-Brynaert J. Surface functionalization of PEEK films using photochemical routes. European Polymer Journal. 2001;**37**:9–18. doi:10.1016/S0014-3057(00)00094-X.

[6] Shi H, Sinke J, Benedictus R. Surface modification of PEEK by UV irradiation for direct co-curing with carbon fibre reinforced epoxy prepregs. International Journal of Adhesion & Adhesives. 2017;**73:**51–57. doi:10.1016/j.ijadhadh.2016.07.017.

[7] Charest J L, Eliason M T, García A J, King W P. Combined microscale mechanical topography and chemical patterns on polymer cell culture substrates. Biomaterials, 2006;**27**(11): 2487–2494. doi:10.1016/j.biomaterials.2005.11.022.

[8] Anselme K, Linez P, Bigerelle M, Noel B, Dufresne E, Judas D, Iost, A, Hardouin P. Qualitative and quantitative study of human osteoblast adhesion on materials with various surface roughnesses. Journal of Biomedical Materials Research.2000;**49**(2): 155–166. doi:10.1002/(SICI)1097-4636(200002)49:2<155::AID-JBM2>3.0.CO;2-J.

[9] Du Y W, Zhang L N, Hou Z T, Ye X, Gu H S, Yan G P, Shang P. Physical modification of polyetheretherketone for orthopedic implants. Frontiers Materials Science. 2014;**8**(4):313–324. doi:10.1007/s11706-014-0266-4.

[10] Besra L, Liu M. A review on fundamental and application of electrophoretic deposition (EPD). Progress in Materials Science. 2007; 52(1):1–61. doi:10.1016/j.pmatsci.2006.07.001.

[11] Boccaccini A R, Roether J A, Thomas B J C, Shaffer M S P, Chavez E, Stoll E, Minay E J. The electrophoretic deposition of inorganic nanoscaled materials. Journal of the Ceramic Society of Japan. 2003; **114**(1):1–14. doi:10.2109/jcersj.114.1.

[12] De Riccardis M F. Ceramic coatings obtained by electrophoretic deposition: Fundamentals, models, post-deposition processes and applications. In: Feng Shi editor. Ceramic coatings: Applications in engineering. Croatia: InTech;2012, pp. 43–68. doi:10.5772/29435.

[13] Corni I, Ryan M P, Boccaccini A R. Electrophoretic deposition: From traditional ceramics to nanotechnology. Journal of the American Ceramic Society. 2008;**28**(7): 1353–1367. doi:10.1016/j.jeurceramsoc.2007.12.011.

[14] Van der Biest O, Vandeperre L J. Electrophoretic deposition of materials. Annual Review Material Science. 1999; **29**:327–352. doi:10.1146/annurev.matsci.29.1.327.

[15] Lewis J A. Colloidal processing of ceramics. Journal of the American Ceramic Society. 2000;**83**: 2341–2359. doi:10.1111/j.1151-2916.2000.tb01560.x.

[16] De Riccardis M F, Carbone D, Rizzo A. A novel method for preparing and characterizing alcoholic EPD suspensions. Journal of Colloid and Interface Science. 2007;307: 109–115. doi:10.1016/j.jcis.2006.10.037.

[17] Sarkar P, Nicholson P S. Electrophoretic deposition (EPD): Mechanisms, kinetics, and application to ceramics. Journal of the American Ceramic Society. 1996;**8**:1987–2002. doi:10.1111/j.1151-2916.1996.tb08929.x.

[18] Voss H, Friedrich K. On the wear behaviour of short-fibre-reinforced PEEK composite. Wear. 1987;**116**:1–18. doi:10.1016/0043-1648(87)90262-6.

[19] Flock J, Friedrich K, Yuan Q. On the friction and wear behaviour of PAN- and pitch-carbon fiber-reinforced PEEK composites. Wear.1999; **229**:304–311. doi:10.1016/S0043-1648(99)00022-8.

[20] Werner P, Altstadt V, Jaskulka R, Jacobs O, Sandler J K W, Shaffer M S P, Windle A H. Tribological behaviour of carbon-nanofibre-reinforced poly(ether ether ketone). Wear. 2004; **257**:1006–1014. doi:10.1016/j.wear.2004.07.010.

[21] Zhang G, Li W-Y, Cherigui M, Zhang C, Liao H, Bordes J M, Coddet C. Structures and tribological performances of PEEK (poly-ether-ether-ketone)-based coatings designed for tribological application. Progress in Organic Coatings. 2007;**60**:39–44. doi:10.1016/j.porgcoat.2007.06.004.

[22] Burris D L, Sawyer W G. Tribological behavior of PEEK components with compositionally graded PEEK/PTFE surfaces. Wear. 2007;**262**:220–224. doi:10.1016/j.wear.2006.03.045.

[23] Wang C, Ma J, Cheng W. Formation of polyetheretherketone polymer coating by electrophoretic deposition method. Surface and Coatings Technology. 2003;**173**:271–275. doi:10.1016/S0257-8972(03)00626-1.

[24] Corni I, Neumann N, Eifler D, Boccaccini A R. Polyetheretherketone (PEEK) coatings on stainless steel by electrophoretic deposition. Advanced Engineering Materials. 2008;**10**: 559–564. doi:10.1002/adem.200800010.

[25] Corni I, Neumann N, Novak S, König K, Veronesi P, Chen Q, Ryan M P, Boccaccini A R. Electrophoretic deposition of PEEK-nano alumina composite coatings on stainless steel. Surface and Coatings Technology. 2009;**203**:1349–1359. doi:10.1016/j.surfcoat.2008.11.005.

[26] Martina V, De Riccardis M F, Carbone D. A chemometric study of alumina/PEEK and hydroxyapatite/PEEK suspensions prepared for electrophoretic deposition of multifunctional coatings. Advances in Science and Technology. 2010;**66**:29–34. doi:10.4028/www.scientific.net/AST.66.29.

[27] Zhang D, Dong G, Chen Y, Zeng Q. Electrophoretic deposition of PTFE particles on porous anodic aluminium oxide film and its tribological properties. Applied Surface Science. 2014;**290**:466–474. doi:10.1016/j.apsucs.2013.11.114.

[28] Jang JH, Machida K, Kim Y, Naoi K. Electrophoretic deposition (EPD) of hydrous ruthenium oxides with PTFE and their supercapacitor performances. Electrochimica Acta. 2006;**52**:1733–1741. doi:10.1016/j.electacta.2006.01.075.

[29] De Riccardis M F, Martina V, Carbone D. Study of polymer particles suspensions for electrophoretic deposition. Journal of Physical Chemistry B. 2013;**117**(6):1592–1599. doi:10.1021/jp3051752.

[30] Boccaccini A R, Keim S, Ma R, Li Y, Zhitomirsky I. Electrophoretic deposition of biomaterials. Journal of the Royal Society Interface. 2010;**7**:S581–S613. doi:10.1098/rsif.2010.0156.focus.

[31] De Riccardis M F, Carbone D, Cuna D. Electrophoretic deposition of lignin reinforced polymer coatings. Key Engineering Materials. 2015;**654**:247–251. doi:10.4028/www.scientific.net/KEM.654.247.

[32] Barsoukov E, Macdonald J R. Impedance spectroscopy: Theory, experiment, and applications. 2nd ed. Hoboken, NJ: Wiley; 2005. ISBN 978-0-471-64749-2.

[33] Orazem M E, Tribollet B. Electrochemical impedance spectroscopy. Hoboken, NJ: John Wiley & Sons; 2008. doi:10.1002/9780470381588.

[34] Lasia A. Electrochemical impedance spectroscopy and its applications. New York: Springer-Verlag; 2014. ISBN 978-1-4614-8933-7.

[35] Bard A J, Faulkner L R. Electrochemical methods: Fundamentals and applications, 2nd ed. Hoboken, NJ: John Wiley & Sons; 2000. ISBN 978-0-471-04372-0.

[36] De Riccardis M F, Carbone D, Capodieci L. Electrophoretically deposited polymeric films: Evidence of correlation between electrochemical impedance spectroscopy measurements and morphological properties. Journal of the Electrochemical Society. 2015;**162:** D3071–D3076. doi:10.1149/2.0201511jes.